ELSEVIER

Vibrational Spectroscopy 30 (2002) 213–225

VIBRATIONAL SPECTROSCOPY

www.elsevier.com/locate/vibspec

Vibrational spectra and structure of 1-phenyltetrazole and 5-chloro-1-phenyltetrazole
A combined study by low temperature matrix isolation and solid state FTIR spectroscopy and DFT calculations

Susana C.S. Bugalho[a], Leszek Lapinski[a], M. Lurdes S. Cristiano[b], Luís M.T. Frija[b], Rui Fausto[a,*]

[a]*Department of Chemistry (CQC), University of Coimbra, 3004-535 Coimbra, Portugal*
[b]*Department of Chemistry, University of Algarve, 8000-117 Faro, Portugal*

Received 15 February 2002; received in revised form 4 April 2002; accepted 4 April 2002

Abstract

Infrared spectra of 1-phenyltetrazole ($C_7N_4H_6$) and 5-chloro-1-phenyltetrazole ($C_7N_4H_5Cl$) isolated in argon matrixes ($T = 8$ K) and in the solid state (at room temperature) were studied. DFT(B3LYP)/6-31G* calculations predict the minimum energy conformation of 1-phenyltetrazole as being non-planar, with the two rings (phenyl and tetrazole) twisted by 29°. For 5-chloro-1-phenyltetrazole, the optimized dihedral angle between the two rings is larger (48°). The theoretically calculated IR spectra of both compounds fit well the spectra observed experimentally. This allowed a reliable assignment of observed IR absorption bands.
© 2002 Elsevier Science B.V. All rights reserved.

Keywords: Tetrazoles; Antiallergic; Myoglobin

1. Introduction

Tetrazole (CN_4H_2) [1] and its derivatives are compounds that have drawn the attention of many people, due to their practical applications. The tetrazolic acid fragment, $–CN_4H$, has similar acidity to the carboxylic acid group, $–CO_2H$, and is almost isosteric with it, but is metabolically more stable [2]. Hence, replacement of $–CO_2H$ groups by $–CN_4H$ groups in biologically active molecules has been widely applied in research areas of major interest [3].

The earlier medicinal applications of tetrazoles have been reviewed [4–6]. As judged by the number of recent patent claims and publications, medicinal uses of tetrazoles continue to grow rapidly, covering a wide range of applications. The tetrazole ring has been used to modify the heme environmental structure of myoglobin by incorporating the *N*-tetrazol-5-yl histidine unit in which the tetrazole ring was formed from the *N*-cyano compound and azide ion [7]. A wide range of tetrazole derivatives has been patented for antihypertension activity and as angiotensin II receptor antagonists. These are claimed to be useful for treating congestive heart failure and preventing cardiac hypertrophy. The tetrazole ring features also in a series of antiallergic substances which act by inhibiting the

* Corresponding author. Tel.: +351-239-827703; fax: +351-239-852080.
E-mail address: rfausto@ci.uc.pt (R. Fausto).

0924-2031/02/$ – see front matter © 2002 Elsevier Science B.V. All rights reserved.
PII: S0924-2031(02)00028-0

allergic histamine release. The 3′-tetrazolo-3′-deoxythymidines are actually the only approved drugs for AIDS treatment, [8,9] while several tetrazole derivatives have been explored for antituberculotic activity. Besides, a wide range of compounds with the tetrazol-1-yl acetic acid structure has been claimed as aldose reductase inhibitors for treatment and prevention of diabetes complications.

Tetrazoles found also application as artificial sweeteners, in agriculture (as plant growth regulators, herbicides and fungicides) [10] and in photography [11]. Another important application of tetrazoles is as gas-generating agents for airbags [12].

Since we are particularly interested to study 5-allyloxy ethers derived from tetrazole, which have demonstrated important practical uses, [13] 5-chloro-1-phenyltetrazole appears as an important molecule to be studied, as it is the main reagent in the ethers synthesis [14].

Due to its electron-withdrawing properties, 5-chloro-1-phenyltetrazole has been extensively used as a derivatizing agent for phenols, prior to conversion into the corresponding arenes [15] through catalytic hydrogenolysis over palladium on charcoal, using hydrogen donors, or into alkyl arenes, [16] through cross-coupling using zinc or tin organometalics. The withdrawal of electron density from the original phenolic C–OH partial double bond on conversion into a tetrazolyl ether weakens it so that it becomes like a C–O single bond in aliphatic alcohols or ethers. The effect at the original phenol is as if the electronegativity of the oxygen increases so much that it becomes similar to that of fluorine [17]. Thus, the heteroaromatic tetrazole, together with the oxygen from the original phenol, acts as an excellent leaving group in catalyzed ipso-substitutions. It has also been reported that selective hydrogenolysis of the C–OH bond in allyl alcohols [18] could be conveniently achieved by first reacting the alcohol with 5-chloro-1-phenyltetrazole so as to form the heteroaromatic allyl ether, which then will undergo smooth heterogeneously catalyzed transfer hydrogenolysis to form the arene corresponding to the aryl or allyl group, and water-soluble phenyltetrazolone. Selective transfer reduction of allyloxytetrazoles is remarkable because it competes with hydrogenation of the double bond [19] and also with the relatively easy Claisen-type sigmatropic rearrangement [20].

Since no works have been denoted so far to investigation of 5-chloro-1-phenyltetrazole and 1-phenyltetrazole molecules in conditions where the interaction with environment are minimized, we decided to study the monomers of these compounds using the matrix isolation technique. A combined (infrared spectroscopy/DFT calculations) approach has been employed in this study.

2. Experimental and computational methods

5-Chloro-1-phenyltetrazole used in this study was a commercial product (Aldrich). 1-Phenyltetrazole was synthesized according to the following procedure. Palladium on charcoal (10%; 1.6 g) was added to a solution of 5-chloro-1-phenyltetrazole (6 g; 33.2 mmol) in toluene (250 ml). The mixture was stirred vigorously and sodium phosphinate (28 g, 264 mmol) was added to it in small amounts, over a period of 2 h. The final mixture was stirred at 40 °C until disappearance of the starting tetrazole was observed by TLC (12 h). The reaction mixture was then filtered through Celite to remove the catalyst and the reaction product extracted with dichloromethane (2 ml × 150 ml). The organic extract was dried over anhydrous sodium sulphate, filtered and evaporated to dryness. The final residue was recrystallised from ethanol to give colorless needles of 1-phenyltetrazole. This sample has been purified by vacuum sublimation prior to matrix-isolation experiments.

The matrix-isolation experiments were carried out with the system built on the basis of an APD cryogenics close-cycle helium refrigeration system with a DE-202A expander. A glass vacuum system and standard manometric procedures were used to deposit the matrix gas (argon, Air Liquid, 99.9999%) using a deposition rate of ca. 10 mmol h^{-1}. 5-Chloro-1-phenyltetrazole or 1-phenyltetrazole were co-deposited from an electrically heated miniature oven placed inside the vacuum chamber of the cryostat [21]. Infrared spectra in the range 4000–500 cm^{-1} were obtained using a Mattson Infinity 60AR FT-spectrometer equipped with a DTGS detector and a Ge/KBr beam splitter. Data collections were performed with 0.5 cm^{-1} spectral resolution. Infrared spectra of solid polycrystalline 5-chloro-1-phenyltetrazole and 1-phenyltetrazole were recorded at room temperature for the compounds pressed in a KBr pellet.

The geometries of 5-chloro-1-phenyltetrazole and 1-phenyltetrazole molecules were optimized using the density functional theory method with the 3 parameters Beck, Yang and Lee functional [22–24] and the 6-31G* basis set [25]. Subsequently, the harmonic vibrational frequencies and IR intensities were calculated at the same level of theory. All the calculations were carried out using the GAUSSIAN 98 program package [26]. In order to correct for anharmonicity and neglected part of electron correlation the calculated frequencies were scaled down by a single factor of 0.975 [27]. A set of internal coordinates was defined and the Cartesian force constants were transformed to the internal coordinates space, allowing ordinary normal-coordinate analysis to be performed as described by Schachtschneider [28]. Internal coordinates used in these calculations are given in Table 1.

3. Results and discussion

DFT(B3LYP)/6-31G* optimized geometries of 1-phenyltetrazole and 5-chloro-1-phenyltetrazole (Fig. 1) are compared with the available experimental X-ray crystallography data in Table 2. As seen in this table, all experimental geometrical parameters are well reproduced by the theoretical calculations.

At optimized geometries the phenyl and tetrazole rings are virtually planar for both studied compounds. The calculated values of the dihedral angle between the planes of the two rings (looking along the C6-N1 axis) is considerably larger for 5-chloro-1-phenyltetrazole (48°) than for 1-phenyltetrazole (29°). The last angle in 1-phenyltetrazole is somewhat (11.8°) [29] greater than the experimental data measured for compound in the crystalline state, but this difference may be attributed to the intermolecular forces stabilizing the crystal. For isolated molecules, there are two main factors determining the dihedral angle between the phenyl and tetrazole rings: stabilization by conjugation of the π electron systems of the two rings, which favors their coplanarity, and minimization of the repulsion of hydrogen atoms (or hydrogen and chlorine atoms) attached to the rings at 5 and 11 positions, which favors non-planar relative orientations. Hence, the larger dihedral angle between the two rings predicted for 5-chloro-1-phenyltetrazole can be easily correlated with the repulsion effect due to the bigger chlorine atom, when compared with that due to the repulsions involving the two hydrogen atoms in 1-phenyltetrazole.

The importance of the size of the *ortho*-substituents to the inter-ring C–C bond in molecules with two connected rings in determining the relative orientation of the rings has been considered for several systems [30–41]. For example, the inter-ring twisting angle in 2-phenylpyridine, where only a single H···H inter-ring repulsion exists, was determined to be 20.7°, while in both 3-phenylpyridine and 4-phenylpyridine, which show two *ortho*-H···H inter-ring repulsions, this angle was estimated to be 38.5 and 36.3°, respectively [33]. In a similar way, the inter-ring twisting angle in 2-phenylimidazole and 2-phenylbenzimidazole was determined to be ca. 20°, while in their analogues bearing an *ortho*-methyl group, 1-methyl-2-phenylimidazole and 1-methyl-2-phenylbenzimidazole, the

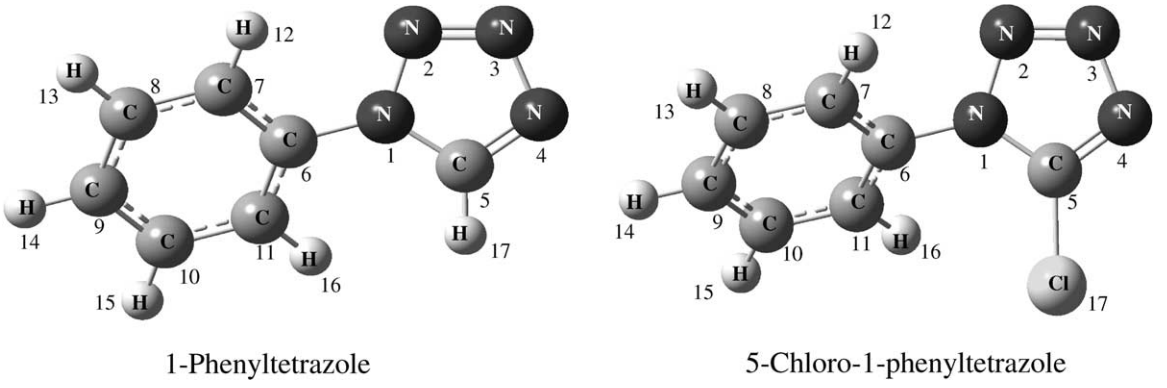

Fig. 1. B3LYP/6-31G* optimized structures for 1-phenyltetrazole and 5-chloro-1-phenyltetrazole, with atom numbering scheme.

Table 1
Definition of internal coordinates used in the normal mode analysis of the 5-chloro-1-phenyltetrazole and 1-phenyltetrazole[a]

Coordinate	Approximate description[b]	Definition[c]
S_1	ν(N2 = N3)	$\nu_{2,3}$
S_2	ν(N4 = C5)	$\nu_{4,5}$
S_3	ν(N1-C5)	$\nu_{1,5}$
S_4	ν(N1-C6)	$\nu_{1,6}$
S_5	ν(C5X)	$\nu_{5,17}$
S_6	ν(N-N)sym	$\nu_{2,1} + \nu_{3,4}$
S_7	ν(N-N)asym	$\nu_{2,1} - \nu_{3,4}$
S_8	ν(C6C7)	$\nu_{6,7}$
S_9	ν(C6C11)	$\nu_{6,11}$
S_{10}	ν(C7H)	$\nu_{7,12}$
S_{11}	ν(C8C9)	$\nu_{8,9}$
S_{12}	ν(C8H)	$\nu_{8,13}$
S_{13}	ν(C9C10)	$\nu_{9,10}$
S_{14}	ν(C9H)	$\nu_{9,14}$
S_{15}	ν(C10H)	$\nu_{10,15}$
S_{16}	ν(C11H)	$\nu_{11,16}$
S_{17}	ν(C–C)sym	$\nu_{7,8} + \nu_{10,11}$
S_{18}	ν(C–C)asym	$\nu_{7,8} - \nu_{10,11}$
S_{19}	δ(R1)	$\delta_{11,6,7} - \delta_{6,7,8} + \delta_{7,8,9} - \delta_{8,9,10} + \delta_{9,10,11} - \delta_{10,11,6}$
S_{20}	δ(R2)	$\delta_{6,7,8} - \delta_{7,8,9} + \delta_{9,10,11} - \delta_{10,11,6}$
S_{21}	δ(R3)	$2\delta_{11,6,7} - \delta_{6,7,8} - \delta_{7,8,9} + 2\delta_{8,9,10} - \delta_{9,10,11} - \delta_{10,11,6}$
S_{22}	τ(R1)	$\tau_{11,6,7,8} - \tau_{6,7,8,9} + \tau_{7,8,9,10} - \tau_{8,9,10,11} + \tau_{9,10,11,6} - \tau_{10,11,6,7}$
S_{23}	τ(R2)	$\tau_{11,6,7,8} - \tau_{7,8,9,10} + \tau_{8,9,10,11} - \tau_{10,11,6,7}$
S_{24}	τ(R3)	$-\tau_{11,6,7,8} + 2\tau_{6,7,8,9} - \tau_{7,8,9,10} - \tau_{8,9,10,11} + 2\tau_{9,10,11,6} - \tau_{10,11,6,7}$
S_{25}	δ(Rr1)	$\delta_{11,6,1} - \delta_{7,6,1} + \delta_{5,1,6} - \delta_{2,1,6}$
S_{26}	δ(Rr2)	$\delta_{11,6,1} - \delta_{7,6,1} - \delta_{5,1,6} + \delta_{2,1,6}$
S_{27}	γ(Rr1)	$\gamma_{1,6,11,7} + \gamma_{6,1,5,2}$
S_{28}	γ(Rr2)	$\gamma_{1,6,11,7} - \gamma_{6,1,5,2}$
S_{29}	τ(Rr)	$\tau_{11,6,1,2} + \tau_{11,6,1,5} + \tau_{7,6,1,2} + \tau_{7,6,1,5}$
S_{30}	δ(r1)	$\delta_{1,2,3} - 0.809\delta_{2,3,4} - 0.809\delta_{5,1,2} + 0.309\delta_{3,4,5} + 0.309\delta_{4,5,1}$
S_{31}	δ(r2)	$-1.118\delta_{2,3,4} + 1.118\delta_{5,1,2} + 1.809\delta_{3,4,5} - 1.809\delta_{4,5,1}$
S_{32}	τ(r1)	$0.309\tau_{1,2,3,4} + 0.309\tau_{5,1,2,3} - 0.809\tau_{2,3,4,5} - 0.809\tau_{4,5,1,2} + \tau_{3,4,5,1}$
S_{33}	τ(r2)	$-1.118\tau_{4,5,1,2} + 1.118\tau_{2,3,4,5} + 1.809\tau_{5,1,2,3} - 1.809\tau_{1,2,3,4}$
S_{34}	δ(CH1)	$\delta_{12,7,6} - \delta_{12,7,8} + \delta_{13,8,7} - \delta_{13,8,9} + \delta_{15,10,9} - \delta_{15,10,11} + \delta_{16,11,10} - \delta_{16,11,6}$
S_{35}	δ(CH2)	$\delta_{12,7,6} - \delta_{12,7,8} + \delta_{13,8,7} - \delta_{13,8,9} - \delta_{15,10,9} + \delta_{15,10,11} - \delta_{16,11,10} + \delta_{16,11,6}$
S_{36}	δ(CH3)	$\delta_{12,7,6} - \delta_{12,7,8} - \delta_{13,8,7} + \delta_{13,8,9} + \delta_{15,10,9} - \delta_{15,10,11} - \delta_{16,11,10} + \delta_{16,11,6}$
S_{37}	δ(CH4)	$\delta_{12,7,6} - \delta_{12,7,8} - \delta_{13,8,7} + \delta_{13,8,9} - \delta_{15,10,9} + \delta_{15,10,11} + \delta_{16,11,10} - \delta_{16,11,6}$
S_{38}	δ(C9H)	$\delta_{14,9,8} - \delta_{14,9,10}$
S_{39}	γ(C7H)	$\gamma_{12,7,6,8}$
S_{40}	γ(C8H)	$\gamma_{13,8,7,9}$
S_{41}	γ(C9H)	$\gamma_{14,9,8,10}$
S_{42}	γ(C10H)	$\gamma_{15,10,9,11}$
S_{43}	γ(C11H)	$\gamma_{16,11,10,6}$
S_{44}	δ(C5X)	$\delta_{17,5,1} - \delta_{17,5,4}$
S_{45}	γ(C5X)	$\gamma_{17,5,1,4}$

[a] ν: stretching; δ: bending; γ: wagging; τ: torsion.

[b] X=H for 1-phenyltetrazole; X=Cl for 5-chloro-1-phenyltetrazole.

[c] $\nu_{i,j}$ is the distance between atoms A_i and A_j; $\delta_{i,k,j}$ the angle between vectors A_iA_j and A_jA_k; $\tau_{i,j,k,l}$ the dihedral angle between the plane defined by A_i, A_j, A_k and the plane defined by A_j, A_k, A_l atoms; $\gamma_{i,j,k,l}$ the angle between the vector A_iA_k and the plane defined by atoms A_j, A_k, A_l (Fig. 1 for atom numbering).

Table 2
B3LYP/6-31G* calculated molecular geometries and available experimental data for 1-phenyltetrazole and 5-chloro-1-phenyltetrazole[a]

	Experimental 1-phenyltetrazole[b]	Calculated B3LYP/6-31G*	
		1-Phenyltetrazole	5-Chloro-1-phenyltetrazole
Bond lengths			
C5-N1	1.344(2)	1.353	1.357
C5-N4	1.302(2)	1.310	1.310
C6-N1	1.431(2)	1.420	1.420
N1-N2	1.348(2)	1.360	1.360
N2-N3	1.298(2)	1.290	1.290
N4-N3	1.354(2)	1.360	1.360
Bond angles			
N1-C5-N4	109.6(1)	109.3	109.9
C7-C6-N1	118.0(1)	119.2	118.4
C11-C6-N1	119.8(1)	119.8	120.3
C5-N1-C6	130.6(1)	130.8	132.3
C5-N1-N2	107.3(1)	107.3	106.5
C6-N1-N2	122.1(1)	121.9	121.1
N1-N2-N3	106.6(1)	106.4	106.9
C5-N4-N3	105.8(1)	105.6	105.2
N2-N3-N4	110.7(1)	111.3	111.5
Dihedral angles			
C7-C6-N1-N2	−11.2(1)	−28.9	−45.7
C11-C6-N1-C5	−12.8(1)	−29.7	−49.2
C7-C6-N1-C5	166.8(2)	150.3	132.2
C11-C6-N1-N2	169.1(2)	151.2	133.0
N4-C5-N1-C6	−179.1(2)	−179.4	−178.3
N4-C5-N1-N2	−0.8(1)	−0.1	−0.3
N1-C5-N4-N3	0.7(1)	0.06	0.2
N1-C6-C7-C8	179.6(2)	−179.7	179.0
N1-C6-C11-C10	−179.6(2)	179.0	−179.6
C5-N1-N2-N3	0.5(1)	0.2	0.2
C6-N1-N2-N3	179.0(2)	179.5	178.6
N1-N2-N3-N4	0.0(1)	−0.1	−0.1
C5-N4-N3-N2	−0.4(1)	0.02	−0.07

[a] Bond lengths in Å; angles in degrees; see Fig. 1 for atom numbering.
[b] Determined by X-ray diffraction for the crystalline compound [29].

twisting angle was found to be 32.3° and 42°, respectively [34]. When considerably large *ortho*-substituents are present, the inter-ring twisting angle may increase substantially, as it is in 4,6-dichloro-2-methylthio-5-phenylpyrimidine, where this angle was found to be ca. 78° [35].

It is also interesting to compare the results obtained now for the two molecules in question with those available for biphenyl [30–32]. The coupling between the two benzene rings in biphenyl is known to be weak and the inter-ring twisting angle varies according to the physical state of the compound, i.e. 0° (planar) in the crystalline state, [30] 19–26° in the liquid state, [31] and ≈40° in the gaseous phase [31,32]. Similar results were found for a series of 1-arylimidazoles, [36] where the inter-ring twisting angle observed in the crystalline phases was found to be systematically smaller than the value predicted for the isolated monomeric species. All these results indicate that intermolecular forces are responsible for the stabilization of more planar structures (smaller inter-ring twisting angles) in the solid state. On the other hand, more twisted structures are assumed under conditions where the relevant intermolecular forces are absent or very

Table 3
B3LYP/6-31G* calculated molecular geometries, rotational constants, dipole moments and Mülliken atomic charges for 1H-tetrazole and 1-phenyltetrazole[a]

	1H-tetrazole	1-Phenyltetrazole
Bond lengths		
C5-N1	1.347	1.353
C5-N4	1.315	1.310
H6/C6-N1	1.011	1.420
N1-N2	1.353	1.360
N2-N3	1.292	1.290
N4-N3	1.366	1.360
Rotational constants		
A	10496.58	3669.99
B	10308.21	711.46
C	5200.77	607.27
Mülliken charges		
N1	−0.549	−0.389
N2	−0.027	−0.066
N3	−0.064	−0.081
N4	−0.359	−0.322
C5	0.306	0.315
C6/H6	0.433	0.289
H7	0.260	0.156
Dipole moment		
μ	5.34	6.05

[a] Bond lengths in Å; rotational constants in MHz; energies in kJ mol^{-1}; charges in units of electron ($e = 1.6021892 \times 10^{-19}$ C); dipole moments in Debyes (1 Debye $= 3.33564 \times 10^{-30}$ Cm) see Fig. 1 for atom numbering.

Table 4
B3LYP/6-31G* calculated molecular geometries, rotational constants, dipole moments and Mülliken atomic charges for 5-chloro-1H-tetrazole and 5-chloro-1-phenyltetrazole[a]

	5-Chloro-1H-tetrazole	5-Chloro-1-phenyltetrazole
Bond lengths		
C5-N1	1.349	1.357
C5-N4	1.312	1.310
H6/C6-N1	1.011	1.420
N1-N2	1.352	1.360
N2-N3	1.294	1.290
N4-N3	1.365	1.360
Rotational constants		
A	10345.18	1558.56
B	2163.25	609.73
C	1789.13	471.56
Mülliken charges		
N1	−0.422	−0.389
N2	−0.031	−0.055
N3	−0.076	−0.077
N4	−0.298	−0.303
C5	0.349	0.328
C6/H6	0.377	0.255
Cl7	0.102	0.095
Dipole moment		
μ	4.64	5.81

[a] Bond lengths in Å; rotational constants in MHz; energies in kJ mol^{-1}; charges in units of electron ($e = 1.6021892 \times 10^{-19}$ C); dipole moments in Debyes (1 Debye $= 3.33564 \times 10^{-30}$ Cm) see Fig. 1 for atom numbering.

weak, as it is the case for molecules isolated in low temperature inert gas matrixes. Hence, it was not expected that the conformations assumed by 1-phenyltetrazole and 5-chloro-1-phenyltetrazole isolated in the matrixes would differ appreciably from the theoretically predicted structures for the isolated molecules in vacuum. As it will be stressed later on in this article, the spectroscopic data obtained in the present study clearly confirmed this hypothesis.

Bond lengths and calculated Mulliken atomic charges on the atoms of the tetrazole ring are compared, for the studied molecules and their parent molecules, 1H-tetrazole [1] and 5-chloro-1H-tetrazole [42], in Tables 3 and 4. Noteworthy, the phenyl-substituted compounds show a reduced tetrazole ring aromaticity, as measured by the bond lengths of the formally single and double bonds (the first are longer and the last shorter in the phenyl substituted compounds than in the corresponding unsubstituted molecules). In the case of 1-phenyl-tetrazole, the phenyl group acts as an electron withdrawing substituent. On the whole, the total electron charge of the tetrazole ring reduces by 0.151 *e*. This charge migration results mainly from the through-space field charge repulsion between H16 (phenyl) and H17 (tetrazole) atoms, since the positive charge of H17 reduces by 0.104 *e*, when compared with that of the equivalent atom in 1H-tetrazole. On the other hand, in 5-chloro-1-phenyltetrazole this effect cannot operate so efficiently, since H16 is now close to the chlorine atom, and so, all changes in the charges due to the 1H → 1-phenyl substitution are much less pronounced than in the previous molecule. On the whole, the presence of the phenyl group leads only to a slight increase of the electron density in the tetrazole ring by 0.018 *e*. All these results, together with the observed non-coplanarity of the phenyl and tetrazole rings, are

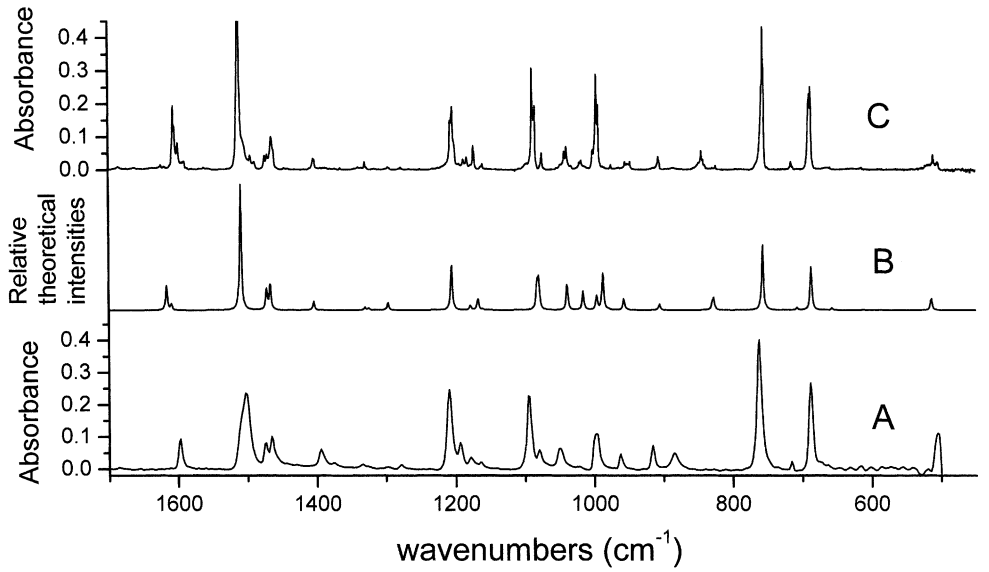

Fig. 2. Infrared absorption spectra of 1-phenyltetrazole: (A) polycrystalline sample in a KBr pellet at room temperature; (B) calculated (B3LYP/6-31G*); (C) matrix-isolated monomer in an argon matrix at 8 K.

compatible with a relatively small interaction between the π-electron systems of the two rings.

The infrared absorption spectrum of monomeric 1-phenyltetrazole isolated in an Ar matrix is compared in Fig. 2 with the spectrum theoretically predicted for the isolated molecule of this compound. The spectrum of polycrystalline 1-phenyltetrazole is also shown in this figure. Analogous comparisons for 5-chloro-1-phenyltetrazole are made in Fig. 3. In spite of the fact that the molecules in question are comparatively complex, the experimental spectra are quite well reproduced by the theoretical simulations. The overall good agreement between experiment and theory enabled to undertake a reliable assignment of the experimentally observed spectra (Tables 5 and 6). That suggests also strongly that the theoretical predictions regarding the non-coplanarity of the phenyl and tetrazole rings in the monomers are correct for both molecules. In addition, the spectra of the polycrystalline compounds in KBr pellets do not drastically differ from those of monomeric species, indicating that in the studied compounds intermolecular interactions are relatively weak in the crystalline state and, in particular, that in this phase the molecules assume the same conformation found in the matrixes, with non-coplanar phenyl and tetrazole rings.

Despite the obvious differences between the IR spectra of 1-phenyltetrazole and 5-chloro-1-phenyltetrazole, there are several spectral features that appear at nearly the same frequencies in both cases (Fig. 4). As expected, this concerns mostly the bands due to vibrations of the phenyl ring. Indeed, these vibrations are not much affected by substitution in the tetrazole ring (at position 5) of hydrogen atom by chlorine, pointing to a relatively unimportant π-electron delocalisation between the two rings in these molecules. In the frequency range close to 1600 cm^{-1} two bands due to stretching vibrations of the phenyl ring are observed at 1606 and 1600 cm^{-1} (for 1-phenyltetrazole) and at 1604 and 1597 cm^{-1} (for 5-chloro-1-phenyltetrazole). The strongest band in the spectra of the studied compounds (observed at 1512 and 1507 cm^{-1}, respectively) corresponds to concerted in-phase bending vibration of the phenyl C–H bonds. In addition, the phenyl C–H out-of-plane wagging vibrations give also rise to a strong band that is observed in the spectra of the studied compounds at 756 and 760 cm^{-1}, respectively. Finally, two phenyl ring vibrations are observed at 690 and 688 cm^{-1} (1-phenyltetrazole) and at 695 and 685 cm^{-1} (5-chloro-1-phenyltetrazole), the higher frequency band being ascribable, for both compounds, to the δ(R3) vibration and the lower

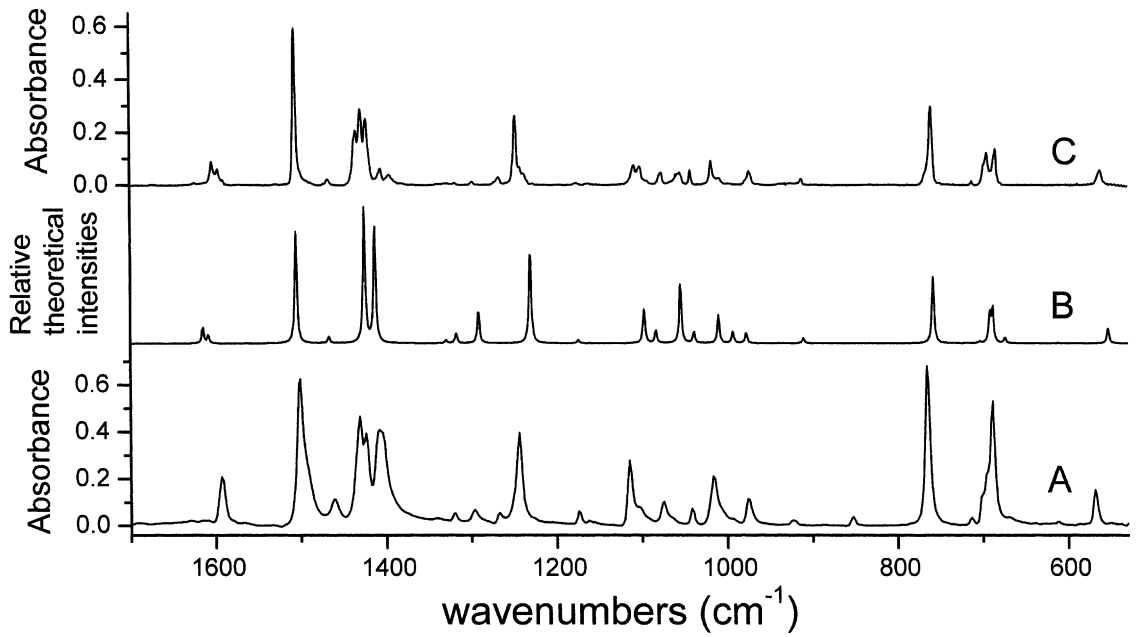

Fig. 3. Infrared absorption spectra of 5-chloro-1-phenyltetrazole: (A) polycrystalline sample in a KBr pellet at room temperature; (B) calculated (B3LYP/6-31G*); (C) matrix-isolated monomer in an argon matrix at 8 K.

Table 5
Calculated and observed frequencies, intensities and potential energy distributions (PED) for 1-phenyltetrazole[a]

Calculated (B3LYP/6-31G*)		Observed			PED[c]
ν(scaled)[b]	I^{ir}	Argon (8.5 K)		Crystal	
		ν	I^{ir}	ν^{ir}	
3222.8	1.5	3170.9		n.o.	ν(C5H) 99
		3155.3			
3154.8	0.2	3123.2		n.o.	ν(C7H) 94
3137.0	8.5	3099.4	31.4	n.o.	ν(C10H) 35, ν(C9H) 30, ν(C11H) 24
3129.1	17.7	3080.2		3123.5	ν(C11H) 42, ν(C8H) 27, ν(C9H) 25
3120.7	6.5	3053.0		3091.3	ν(C8H) 41, ν(C10H) 27, ν(C11H) 25
3112.1	0.3	3037.4		3064.3	ν(C9H) 38, ν(C10H) 34, ν(C8H) 19
1616.4	16.1	1606.2	20.5	1597.3	ν(C–C)sym 49, δ(CH3) 15, δ(R3) 10
		1604.5	sh		
1609.4	3.9	1599.9	5.1	n.o.	ν(C8C9) 20, ν(C9C10) 20, ν(C6C11) 18, ν(C6C7) 17
1509.4	82.1	1511.8	94.5	1501.9	δ(CH2) 42, ν(N1-C6) 13
1472.3	13.2	1474.6	3.7	1474.7	ν(N4=C5) 25, ν(C–C)asym 16, δ(C9H) 15, δ(CH4) 13
		1471.4	2.6		
1466.9	17.5	1464.9	16.5	1465.8	ν(N4=C5) 19, ν(N1-C5) 13, ν(C–C)asym 11, δ(C5H) 11
1404.2	5.7	1404.4	1.5	1394.7	ν(N4=C5) 27, ν(N1-C5) 22, ν(N1-C6) 14
		1403.0	1.5		
1330.4	1.9	1339.9	0.5	1334.6	δ(CH1) 34, ν(C–C)asym 23, δ(C9H) 10
1324.9	1.3	1330.4	1.0	1325.6	ν(N2=N3) 24, δ(CH1) 23
1297.1	5.1	1296.8	0.5	1278.7	ν(N2=N3) 50, δ(CH1) 21
		1295.0	0.2		

Table 5 (*Continued*)

Calculated (B3LYP/6-31G*)		Observed			PED[c]
		Argon (8.5 K)		Crystal	
ν(scaled)[b]	I^{ir}	ν	I^{ir}	ν^{ir}	
1205.5	31.5	1207.0 1203.9	36.3	1209.3 1193.8	ν(N1-C5) 16, δ(r2) 16, δ(C5H) 16, ν(N2=N3) 15, ν(N1-C6) 13
1178.4	3.0	1188.4 1183.5	3.0 3.1	1178.3	δ(CH3) 57, δ(C5H) 14
1167.6	7.7	1173.6	6.0	1163.6	δ(CH3) 25, δ(C–H) 24, ν(N1-C5) 16
1160.4	0.4	1160.8	1.8	n.o.	δ(CH4) 42, δ(C9H) 39
1082.7	16.9	1089.5	38.7	1094.7	δ(r1) 20, δ(CH4) 17, ν(C–C)asym 17, ν(N–N)asym 11
1080.0	18.7	1085.4		1080.5	δ(r1) 31, ν(N–N)asym 17, ν(C–C)asym 15, δ(CH4) 11
		1075.2	4.0		
1039.0	17.5	1042.9 1039.8	13.1	1050.3	δ(CH2) 27, ν(N–N)sym 17, ν(C8C9) 14, ν(C6C11) 12, ν(C9C10) 10
1016.0	12.2	1020.9 1018.2	5.4	1022.1	ν(N–N)sym 39, ν(C8C9) 14, ν(C9C10) 13, δ(R1) 12, ν(C–C)sym 10
		1001.9	sh		δ(R1) 19, ν(C–C)sym 15, ν(C6C11) 13, ν(C6C7) 10
987.3	25.1	996.7	36.3	997.0	δ(R1) 54, ν(N–N)sym 12, δ(r1) 12, δ(r2) 12
996.2	9.0	993.8			
979.5	0.5	975.6	1.2	n.o.	γ(C8H) 43, γ(C9H) 41, γ(C10H) 21, γ(C7H) 13
957.3	7.4	955.3 951.9 947.8	5.2	962.5	δ(r2) 50, ν(N–N)sym 35
952.5	0.3	n.o.		n.o.	γ(C10H) 44, γ(C7H) 27, γ(C8H) 22, γ(C11H) 17
905.9	3.7	907.0	3.8	916.4	γ(C11H) 38, γ(C7H) 32, γ(C9H) 30
830.0	3.8	845.5	9.2	885.0	γ(C5H) 57,γ(C11H) 17,γ(C7H) 12,γ(C8H) 10
827.8	7.2	842.9		n.o.	γ(C5H) 48,γ(C11H) 19,γ(C7H) 15, γ(C8H) 12
756.9	44.1	756.2	48.8	762.5	γ((C9H) 28, γ(C10H) 17, γ(Rr1) 15, γ(C8H) 13, τ(R1) 13
707.3	1.6	715.7	2.0	715.5	τ(r2) 65, τ(r1) 32
687.5	12.5	689.7	16.7	688.3	δ(R3) 42, τ(R1) 19
687.0	16.6	688.0	18.2	n.o.	τ(R1) 73, δ(R3) 12
657.2	1.4	660.0	1.8	n.o.	τ(r1) 61, τ(r2) 26
612.4	0.3	614.4	0.7	n.o.	δ(R2) 86
514.1	7.6	511.2 504.7	9.8	506.2	τ(R2) 33, γ(Rr1) 30, τ(R1) 13
428.7	1.1	n.o.		n.o.	δ(Rr2) 58
406.6	0.05	n.o.		n.o.	τ(R3) 114.8
349.4	1.1	n.o.		n.o.	δ(R3) 35, ν(N1-C6) 32
288.1	2.0	n.o.		n.o.	τ(R2) 57, γ(Rr1) 19, δ(Rr1) 17
148.1	3.7	n.o.		n.o.	δ(Rr1) 73, γ(Rr1) 18
105.4	1.8	n.o.		n.o.	γ(Rr2) 86, τ(R2) 14
49.7	3.7	n.o.		n.o.	τ(Rr) 99

[a] Frequencies in cm^{-1} and ν, stretching; δ, in-plane bending; γ, out-of-plane bending; sym, symmetric; asym, antisymmetric; n.o., not observed. See Fig. 1 for atom numbering. Calculated infrared intensities (I^{ir}) in km mol^{-1}. Intensities of experimental bands were measured by numerical integration, they are scaled in such a manner that the sum of all assigned bands is equal the sum of the intensities of the corresponding, theoretically calculated bands.

[b] Frequencies were scaled by a single factor (0.975).

[c] Only PED contributions larger than 10% are presented.

Table 6
Calculated and observed vibrational frequencies, intensities and PED for 5-chloro-1-phenyltetrazole[a]

Calculated (B3LYP/-31G*)		Observed			PED[c]
ν(scaled)[b]	I^{ir}	Argon (8.5 K)		Crystal	
		ν	I^{ir}	ν^{ir}	
3148.7	0.5	n.o.			ν(C7H) 85, ν(C8H) 10
3144.8	2.3	3118.9	1.6		ν(C11H) 80, ν(C10H) 14
3132.9	16.3	3076.1	12.0	3064.0	ν(C9H) 48, ν(C8H) 21, ν(C10H) 13, ν(C11H) 11
3123.6	8.6	3065.6			ν(C8H) 46, ν(C10H) 45
3113.1	0.05	n.o.			ν(C9H) 48, ν(C10H) 26, ν(C8H) 23
1614.9	8.2	1603.6	12.3		ν(C–C)sym 49, δ(CH3) 15, δ(R3) 10
1608.5	4.1	1596.9	10.4	1592.6	ν(C9C10) 21, ν(C8C9) 19, ν(C6C7) 18, ν(C6C11) 18
		1590.8	0.5		
1505.4	57.5	1506.8	76.0	1501.4	δ(CH2) 48, ν(N1-C6) 10, ν(C6C7) 10
1467.0	3.4	1468.1	3.9	1461.1	ν(C–C)asym 27, δ(C9H) 24, δ(CH4) 21
1425.3	70.3	1435.2	33.7	1431.4	ν(N4 = C5) 51
		1429.5	31.3	1423.6	
1413.1	61.9	1423.2	57.4	1406.8	ν(N1-C5) 35, ν(N4=C5) 17, ν(N1-C6) 13
		1406.4	6.5		
		1396.1	15.1		
1329.6	1.7	1317.9	0.5	1340.1	ν(C–C)asym 27, δ(CH1) 23, ν(C9C10) 11,ν(C8C9) 10
1317.7	5.3	1298.7	1.6	1320.4	δ(CH1) 48, ν(N2=N3) 11
1291.4	17.4	1268.0	3.9	1296.4	ν(N2=N3) 73
				1267.5	
1231.0	50.2	1247.8	42.3	1244.1	ν(N1-C5) 26, ν(N1-C6) 19, δ(r2) 15
		1242.6	sh		
		1237.7	sh		
1174.8	1.7	1176.9	1.0	1173.9	δ(CH3) 83, ν(C–C)sym 11
1161.3	0.1	1163.5	1.3		δ(C9H) 41, δ(CH4) 39
1097.5	18.3	1109.1	13.1	1114.9	ν(N–N)asym 36, δ(r1) 29, δ(CH4) 12
		1102.4	12.8		
1083.5	6.6	1077.3	6.0	1102.9	ν(N–N)sym 19, ν(C–C)asym 19, δ(CH4) 17, ν(N–N)asym 11, δ(r1) 10
1054.7	31.4	1060.0	9.9	1075.6	ν(N–N)sym 68
		1055.5			
1038.7	5.9	1042.7	4.2	1041.7	δ(CH2) 30, ν(C6C7) 13, ν(C6C11) 12, ν(C9C10) 12, ν(C8C9) 12
1010.1	14.5	1018.4	13.1	1016.5	ν(C–C)sym 20, ν(C8C9) 19, ν(C9C10) 16
993.1	6.2	1009.6	2.9	993.4	δ(R1) 76
980.9	0.2	n.o.			γ(C9H) 46, γ(C8H) 35, γ(C10H) 27
977.5	5.3	973.9	8.9	975.0	δ(r2) 44, ν(N–N)asym 24, δ(r1) 20, ν(N1-C5) 13
953.6	0.06	n.o.			γ(C10H) 37, γ(C8H) 30, γ(C7H) 25, γ(C11H) 23
910.6	2.6	912.8	2.1	923.6	γ(C11H) 38, γ(C7H) 35, γ(C9H) 31
830.3	0.08	n.o.		852.8	γ(C11H) 31, γ(C7H) 29, γ(C8H) 21, γ(C10H) 19
758.3	35.1	760.8	48.0	765.2	γ(C9H) 26, γ(C10H) 16, τ(R1) 15, γ(C8H) 14,γ(Rr1) 13
703.5	0.7	712.7	0.8	714.1	τ(r2) 56, τ(r1) 32
691.8	15.3	695.1	21.4	701.6	δ(R3) 41, τ(R1) 16, ν(N1-C6) 10
				695.6	
688.4	17.0	684.9	21.4	689.1	τ(R1) 68, τ(r1) 10
674.1	2.8	678.8	0.08	n.o.	τ(r1) 39, τ(r2) 27, γ(C–Cl) 14
612.1	0.2	n.o.		n.o.	δ(R2) 85
553.3	8.2	562.3	11.2	569.0	ν(C5Cl) 19, δ(Rr2) 17, τ(R1) 13, τ(R2) 11,γ(Rr1) 11
490.6	1.3	n.o.		n.o.	ν(C5Cl) 40, τ(R2) 17, γ(Rr1) 13
445.3	0.5	n.o.		n.o.	δ(Rr2) 24, δ(C–Cl) 19, γ(Rr1) 11
408.8	0.03	n.o.		n.o.	τ(R3) 114

Table 6 (*Continued*)

Calculated (B3LYP/-31G*)		Observed			PED[c]
ν(scaled)[b]	I^{ir}	Argon (8.5 K)		Crystal	
		ν	I^{ir}	ν^{ir}	
361.3	0.6	n.o.		n.o.	δ(R3) 13, τ(R2) 12, δ(C–Cl) 12, ν(N1-C6) 11, δ(Rr1) 11
321.2	2.1	n.o.		n.o.	τ(R2) 26, δ(R3) 15, ν(N1-C6) 14, δ(Rr1) 11
235.8	1.6	n.o.		n.o.	γ(C–Cl) 59, τ(r1) 14
220.3	0.3	n.o.		n.o.	δ(C–Cl) 37, τ(R2) 27, γ(Rr1) 10
113.4	0.8	n.o.		n.o.	δ(Rr1) 38, γ(Rr1) 29, γ(Rr2) 19
90.5	0.5	n.o.		n.o.	γ(Rr2) 66, δ(Rr1) 14, τ(R2) 12
42.8	0.5	n.o.		n.o.	τ(Rr) 92

[a] Frequencies in cm^{-1} and ν, stretching, δ, in-plane bending; γ, out-of-plane bending; sym, symmetric; asym, antisymmetric; n.o., not observed. See Fig. 1 for atom numbering. Calculated infrared intensities (I^{ir}) in km mol^{-1}. Intensities of experimental bands were measured by numerical integration, they are scaled in such a manner that the sum of all assigned bands is equal the sum of the intensities of the corresponding, theoretically calculated bands.

[b] Frequencies were scaled by a single factor (0.975).

[c] Only PED contributions larger than 10% are presented.

frequency feature to τ(R1) (Tables 5 and 6). Indeed, all these bands are well known mark bands for mono-substituted phenyl groups [28].

It is interesting to note that the vibrational data corresponding to the vibrations mainly localized in the tetrazole ring agree with the structural information in what concerns to the above discussed reduction of the aromatic character of the ring upon 1H → 1-phenyl substitution. In fact, in 1-phenyltetrazole bands with the largest contribution of νN2=N3 and νC5=N4 appear at average values of 1296 and 1473 cm^{-1} (both features are observed as doublets) while in 1H-tetrazole the corresponding bands were observed at 1243 and 1468 cm^{-1}, [1] i.e. the spectroscopic data also indicate that these bonds are stronger in the phenyl-substituted compound. On the other hand, νC5-N1 reduces its frequency upon the 1H → 1-phenyl substitution (1428 [1] versus 1404 cm^{-1}), i.e. the C5-N1

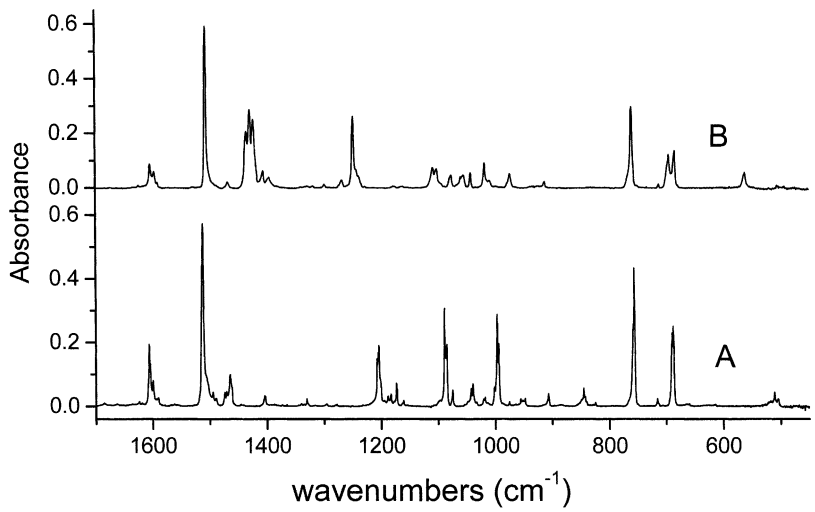

Fig. 4. Comparison of the infrared absorption spectra of 1-phenyltetrazole (A) and 5-chloro-1-phenyltetrazole (B) isolated in argon matrixes ($T = 8$ K).

single bond becomes weaker. Similar findings can also be noticed in the case of the chloro-substituted molecules. For example, νN2=N3 and νC5=N4 appear at 1268 and 1432 cm^{-1} in 5-chloro-1-phenyltetrazole and at 1248 and 1419 cm^{-1} in 5-chlorotetrazole [42].

4. Conclusion

Matrix-isolation infrared spectroscopy supported by theoretical predictions undertaken at the B3LYP/6-31G* level of theory enabled, for the first time, complete characterization of the vibrational signature of monomeric forms of 1-phenyltetrazole and 5-chloro-1-phenyltetrazole. It was also shown that in the gas phase as well as in argon matrixes these two molecules assume non-coplanar arrangements of the phenyl and tetrazole rings, with the chloro-substituted compound showing a larger dihedral angle defined by the planes of the two rings (48° versus 29°; calculated values for the isolated molecule in vacuum). For both compounds, the spectrum of a polycrystalline sample, obtained for the substance in a KBr pellet at room temperature, was found not to differ dramatically from that obtained for the matrix-isolated monomer, indicating that no strong intermolecular interactions are operating in the solid phase. In addition, when compared with the non-substituted 1H-tetrazole molecule and 5-chloro-1H-tetrazole, the 1-phenyl-substituted compounds now studied reveal a smaller aromaticity of their tetrazolic ring.

Acknowledgements

The authors acknowledge the Portuguese Science Foundation (FCT) for financial support (Research projects PRAXIS/P/QUI/10137/1998 and PRAXIS/P/CTM/14185/1998).

References

[1] S.C.S. Bugalho, E.M.S. Maçôas, M.L.S. Cristiano, R. Fausto, Phys. Chem. Chem. Phys. 3 (2001) 3541.
[2] H. Singh, A.S. Chawla, V.K. Kapoor, D. Paul, R.K. Malhotra, Prog. Med. Chem. 17 (1980) 151.
[3] K. Noda, Y. Saad, A. Kinoshita, T.P. Boyle, R.M. Graham, A. Husain, S.S. Karnik, J. Biol. Chem. 270 (1995) 2284.
[4] T. Mavromoustakos, A. Kolocouris, M. Zervou, P. Roumelioti, J. Matsoukas, R. Weisemann, J. Med. Chem. 42 (1999) 1714.
[5] J.H. Toney, P.M.D. Fitzgerald, N. Grover-sharma, S.H. Olson, W.J. May, J.G. Sundelof, D.E. Vanderwall, K.A. Cleary, S.K. Grant, J.K. Wu, J.W. Kozarich, D.L. Pompliano, G.G. Hammond, Chem. Biol. 5 (1998) 185.
[6] Y. Hashimoto, R. Ohashi, Y. Kurosawa, K. Minami, H. Kaji, K. Hayashida, H. Narita, S. Murata, J. Cardiovasc. Pharm. 31 (1998) 568.
[7] A. Desarro, D. Ammendola, M. Zappala, S. Grasso, G.B. Desarro, Antimicrob. Agents Chemother. 39 (1995) 232.
[8] Y. Tamura, F. Watanabe, T. Nakatani, K. Yasui, M. Fuji, T. Komurasaki, H. Tsuzuki, R. Maekawa, T. Yoshioka, K. Kawada, K. Sugita, M. Ohtani, J. Med. Chem. 41 (1998) 640.
[9] A.D. Abell, G.J. Foulds, J. Chem. Soc. Perkin Trans. 1 17 (1997) 2475.
[10] G. Sandmann, C. Schneider, P. Boger, Z. Naturforsch. C 51 (1996) 534.
[11] G.I. Koldobskii, V.A. Ostrovskii, V.S. Poplavskii, Khim. Geterotsikl. Soedin. 10 (1981) 1299.
[12] C. Zhao-Xu, X. Heming, Int. J. Quant. Chem. 79 (2000) 350.
[13] M.L.S. Cristiano, Ph.D. Thesis, University of Liverpool, UK, 1994.
[14] J.K. Elwood, J.W. Gates, J. Org. Chem. 32 (1997) 2956.
[15] R.A.W. Johnstone, P.J. Price, Tetrahedron 41 (1985) 2483.
[16] R.A.W. Johnstone, W.N. McLean, Tetrahedron Lett. 29 (1988) 5553.
[17] J.A.C. Alves, J.V. Barkley, A.F. Brigas, R.A.W. Johnstone, J. Chem. Soc. Perkin Trans. 2 4 (1997) 669.
[18] M.L.S. Cristiano, R.A.W. Johnstone, P.J. Price, J. Chem. Soc. Perkin Trans. 1 12 (1996) 1453.
[19] M.L.S. Cristiano, R.A.W. Johnstone, J. Chem. Soc. Perkin Trans. 2 3 (1997) 489.
[20] M.L.S. Cristiano, R.A.W. Johnstone, J. Chem. Res. (Synopses) 5 (1997) 164.
[21] I.D. Reva, S. Stepanian, L. Adamowicz, R. Fausto, J. Phys. Chem. A 105 (2001) 4773.
[22] A.D. Becke, Phys. Rev. B 38 (1988) 3098.
[23] C. Lee, W. Yang, R.G. Parr, Phys. Rev. B 37 (1988) 785.
[24] S.H. Vosko, L. Wilk, M. Nusair, Can. J. Phys. 58 (1980) 1200.
[25] W.J. Hehre, R. Ditchefield, J.A. Pople, J. Chem. Phys. A 56 (1972) 2257.
[26] M.J. Frisch, G.W. Trucks, H.B. Schlegel, G.E. Scuseria, M.A. Robb, J.R. Cheeseman, V.G. Zakrzewski, J.A. Montgomery Jr., R.E. Stratmann, J.C. Burant, S. Dapprich, J.M. Millam, A.D. Daniels, K.N. Kudin, M.C. Strain, O. Farkas, J. Tomasi, V. Barone, M. Cossi, R. Cammi, B. Mennucci, C. Pomelli, C. Adamo, S. Clifford, J. Ochterski, G.A. Petersson, P.Y. Ayala, Q. Cui, K. Morokuma, D.K. Malick, A.D. Rabuck, K. Raghavachari, J.B. Foresman, J. Cioslowski, J.V. Ortiz, A.G. Baboul, B.B. Stefanov, G. Liu, A. Liashenko, P. Piskorz, I. Komaromi, R. Gomperts, R.L. Martin, D.J. Fox, T. Keith, M.A. Al-Laham, C.Y. Peng, A. Nanayakkara, C. Gonzalez, M. Challacombe, P.M.W. Gill, B. Johnson, W. Chen, M.W. Wong, J.L. Andres, C. Gonzalez, M. Head-Gordon, E.S.

Replogle, J.A. Pople, Gaussian 98, Revision A.7., Gaussian Inc., Pittsburgh, PA, 1998.
[27] D.J. Defrees, A.D. McLean, J. Chem. Phys. A 82 (1985) 333.
[28] J.H. Schachtschneider, Technical Report Shell Development Co., Emeryville, CA, 1969.
[29] T. Matsunaga, Y. Ohno, Y. Akutsu, M. Arai, M. Tamura, M. Iida, Acta Cryst. C 55 (1999) 129.
[30] A. Hargreaves, S.H. Rizvi, Acta Cryst. 15 (1962) 365.
[31] H. Suzuki, Bull. Chem. Soc. Jpn. 32 (1959) 1340.
[32] G.H. Beaven, in: G.W. Gray (Ed.), Steric Effects in Conjugated Systems, Butterworths, London, 1958.
[33] M.A.V. Ribeiro da Silva, M.A.R. Matos, C.A. Rio, V.M.F. Morais, J. Wang, G. Nichols, J.S. Chickos, J. Phys. Chem. A 104 (2000) 1774.
[34] J. Catalán, J.L.G. de Paz, J.C. Del Valle, M. Kasha, J. Phys. Chem. A 101 (1997) 5284.
[35] D.E. Lynch, I. McClenaghan, Acta Cryst. E 57 (2001) 264.
[36] N.H. Damrauer, J.K. McCusker, J. Phys. Chem. A 103 (1999) 8440.
[37] M.K. Cyranski, J. Mieczkowski, Acta Cryst. C 54 (1998) 1521.
[38] J.A. Cowan, J.A.K. Howard, M.A. Leech, Acta Cryst. C 57 (2001) 302.
[39] J. Zucherman-Schpector, E.J. Barreiro, A.C.C. Freitas, Acta Cryst. C 50 (1994) 2095.
[40] A. Kowalski, Acta Cryst. C 51 (1995) 1670.
[41] N.H. Damrauer, B.T. Weldon, J.K. McCusker, J. Phys. Chem. A 102 (1998) 3382.
[42] S.C.S. Bugalho, A.C. Serra, L. Lapinski, M.L. Cristiano, R. Fausto, Phys. Chem. Chem. Phys. 4 (2002) 1725.